Studying of B_{s}^{0}-B[over ¯]_{s}^{0} mixing and B_{s}→K^{(}*^{)-}K^{(}*^{)+} decays within supersymmetry

Ru-Min Wang, Yuan-Guo Xu, Qin Chang, and Ya-Dong Yang

Phys. Rev. D **83**, 095010 — Published 19 May 2011

DOI: 10.1103/PhysRevD.83.095010

Studying of $B_s^0 - \bar{B}_s^0$ mixing and $B_s \to K^{(*)-}K^{(*)+}$ decays within supersymmetry

Ru-Min Wang[1]*, Yuan-Guo Xu[1]†, Qin Chang[2]‡, Ya-Dong Yang[3,4]§

[1] *College of Physics and Electronic Engineering, Xinyang Normal University, Xinyang, Henan 464000, China*

[2] *Department of Physics, Henan Normal University, Xinxiang, Henan 453007, P. R. China*

[3] *Institute of Particle Physics, Huazhong Normal University, Wuhan, Hubei 430079, P. R. China*

[4] *Key Laboratory of Quark & Lepton Physics, Ministry of Education, P.R. China*

Abstract

Recent results from CDF and DØ collaborations favor a large CP asymmetry in $B_s^0-\bar{B}_s^0$ mixing, while the standard model prediction is very small. Such a large phase may imply sizable new physics effects in $B_s^0 - \bar{B}_s^0$ mixing. We compute the gluino-mediated supersymmetry contributions to $B_s^0 - \bar{B}_s^0$ mixing, $B_s \to K^{(*)-}K^{(*)+}$ and $B \to X_s\gamma$ decays in the frame of the mass insertion approximation. Combining the constraints of ΔM_s, $\Delta\Gamma_s$, $\phi_s^{J/\psi\phi}$, $\mathcal{B}(B_s \to K^-K^+)$ and $\mathcal{B}(B \to X_s\gamma)$, we find that the effects of the constrained LL and RR insertions in $B_s \to K^{(*)-}K^{(*)+}$ decays are small because of the absence of gluino mass enhancement. For $m_{\tilde{g}}^2/m_{\tilde{q}}^2 = 9$, the constrained LR insertion can provide sizable contributions to all observables of $B_s \to K^{(*)-}K^{(*)+}$ decays except $\mathcal{A}_{CP}^{dir}(B_s \to K^-K^+)$, and many observables are sensitive to the modulus and the phase of the LR insertion parameter. Near future experiments at Fermilab Tevatron and CERN LHC-b can test these predictions and shrink/reveal the mass insertion parameter spaces.

PACS Numbers: 12.60.Jv, 12.15.Ji, 12.38.Bx, 13.25.Hw

*E-mail: ruminwang@gmail.com

†E-mail: yuanguox@gmail.com

‡E-Mail: changqin@htu.cn

§E-Mail: yangyd@iopp.ccnu.edu.cn

1 Introduction

The flavor changing neutral current (FCNC) processes in the $b \to s$ transition are sensitive to the effects of New Physics (NP) beyond the Standard Model (SM). Recently, both CDF and DØ collaborations have announced their measurements of extracted CP violating phase $\phi_s^{J/\psi\phi}$ associated with $B_s^0 - \bar{B}_s^0$ mixing [1–3]. The CP violating phase measured by both CDF and DØ is $\phi_s^{J/\psi\phi} \in [0.20, 2.84]$ at 95% C.L. [4], which is much larger than its SM value $\phi_s^{J/\psi\phi,\mathrm{SM}} = 2\beta_s^{\mathrm{SM}} \equiv 2\mathrm{arg}\left(-\frac{V_{ts}V_{tb}^*}{V_{cs}V_{cb}^*}\right) \approx 0.04$ [5–9]. More recently, the DØ collaboration has reported evidence for an anomalously large CP violation in the like-sign dimuon charge asymmetry in semileptonic B-hadron decays $A_{sl}^b = (-9.57 \pm 2.51(\mathrm{stat}) \pm 1.46(\mathrm{syst})) \times 10^{-3}$ [10], which differs by 3.2 standard deviations from the SM prediction $A_{sl}^{b,\mathrm{SM}} = (-2.3^{+0.5}_{-0.6}) \times 10^{-4}$ [5, 11]. Although the errors of the data are still large, these deviations from the SM could be attributed to the presence of non-SM flavor violationin the $b \to s, d$ non-leptonic decays.

Recently, the CDF collaboration has made the first measurement of charmless two-body $B_s \to K^-K^+$ decay, $\mathcal{B}(B_s \to K^-K^+) = (26.5 \pm 4.4) \times 10^{-6}$ [9, 12, 13]. The measurement is important for understanding B_s physics, and also implies that many B_s decay modes could be precisely measured at the LHC-b. Comparing with the theoretical predictions for these observables in Refs. [14–16], one would find that the experimental measurements of branching ratio are in agreement with the SM predictions within their large theoretical uncertainties. However, NP effects would be still possible to render other observable deviated from the SM expectation with the branching ratios nearly unaltered [17].

Supersymmetry (SUSY) is an extension of the SM which emerges as one of the promising candidates for NP beyond the SM. In general SUSY, a new source of flavor violation is introduced by the squark mass matrices, which usually can not be diagonalized on the same basis as the quark mass matrices. This means gluinos (and other gaugios) will have flavor-changing couplings to quarks and squarks, which implies the FCNCs could be mediated by gluinos and thus have strong interaction strength. It is customary to rotate the effects so they occur in squark propagators rather than in couplings, and to parameterize them in terms of dimensionless mass insertion (MI) parameters $(\delta_{AB}^{u,d})_{ij}$ with $(A, B) = (L, R)$ and $(i, j = 1, 2, 3)$.

$B_s^0 - \bar{B}_s^0$ mixing, $B_s \to K^{(*)-}K^{(*)+}$ and $B \to X_s\gamma$ decays are all induced by the $b \to s$ transition, and they involve the same set of the MI parameters. Inspired by the recent measurements

from CDF and DØ collaborations , we study $B_s^0 - \bar{B}_s^0$ mixing, $B_s \to K^{(*)-}K^{(*)+}$ and $B \to X_s\gamma$ decays in the usual MI approximation [18, 19] of general SUSY models, where flavor violation due to the gluino mediation can be important. The chargino-stop and the charged Higgs-top loop contributions are parametrically suppressed relative to the gluino contributions, and thus are ignored following [19–22]. Following the similar way to our previous article [23], we consider the LL, RR, LR and RL four kinds of the MIs with $m_{\tilde{g}}^2/m_{\tilde{q}}^2 = 0.25, 1, 4, 9$, respectively. We find that the LL and RR insertions for all cases of $m_{\tilde{g}}^2/m_{\tilde{q}}^2$ values as well as the LR insertion for $m_{\tilde{g}}^2/m_{\tilde{q}}^2 = 9$ case could explain current experimental data simultaneously. For $m_{\tilde{g}}^2/m_{\tilde{q}}^2 = 9$, the constrained LR MI could significantly affect all observables of $B_s \to K^{(*)-}K^{(*)+}$ decays except $\mathcal{A}_{CP}^{dir}(B_s \to K^-K^+)$ without conflict with all related data at 95% C.L.. While the constrained LL and RR insertions from $B_s^0 - \bar{B}_s^0$ mixing have small effects in $B_s \to K^{(*)-}K^{(*)+}$ decays because of the absence of gluino mass enhancement. Therefore, with the ongoing B-physics at Tevatron, in particular with the onset of the LHC-b experiment, we expect a wealth of B_s data and measurements of these observables could restrict or reveal the parameter spaces of the LR (LL and RR) insertions in the near future.

The paper is arranged as follows. In Sec. 2, the relevant formulas for $B_s \to K^{(*)-}K^{(*)+}$ decays and $B_s^0 - \bar{B}_s^0$ mixing are presented. Sec. 3 deals with the numerical results. Using our constrained MI parameter spaces from $B_s \to K^{(*)-}K^{(*)+}$ decay and $B_s^0 - \bar{B}_s^0$ mixing, we explore the MI effects on the other observable observables, which have not been measured yet in $B_s \to K^{(*)-}K^{(*)+}$ decays. Sec. 4 contains our summary and conclusion. Theoretical input parameters are summarized in the Appendix.

2 The theoretical frame

2.1 $B_s \to K^{(*)-}K^{(*)+}$ decays

2.1.1 The decay amplitudes in the SM

In the SM, the effective Hamiltonian for the $b \to su\bar{u}$ transition at the scale $\mu \sim m_b$ is given by [24]

$$\mathcal{H}_{eff}^{SM}(\Delta B = 1) = \frac{G_F}{\sqrt{2}} \sum_{p=u,c} \lambda_p \left(C_1^{SM} Q_1^p + C_2^{SM} Q_2^p + \sum_{i=3}^{10} C_i^{SM} Q_i + C_{7\gamma}^{SM} Q_{7\gamma} + C_{8g}^{SM} Q_{8g} \right) + \text{h.c.}, \quad (1)$$

where $\lambda_p = V_{pb}V_{ps}^*$ with $p \in \{u, c\}$ are CKM factors, the Wilson coefficients within the SM C_i^{SM} can be found in Ref. [24], and the relevant operators Q_i are given as

$$
\begin{aligned}
Q_1^p &= (\bar{p}_\alpha \gamma^\mu L b_\alpha)(\bar{s}_\beta \gamma_\mu L p_\beta), & Q_2^p &= (\bar{p}_\alpha \gamma^\mu L b_\beta)(\bar{s}_\beta \gamma_\mu L p_\alpha), \\
Q_3 &= (\bar{s}_\alpha \gamma^\mu L b_\alpha) \sum_{q'} (\bar{q}'_\beta \gamma_\mu L q'_\beta), & Q_4 &= (\bar{s}_\beta \gamma^\mu L b_\alpha) \sum_{q'} (\bar{q}'_\alpha \gamma_\mu L q'_\beta), \\
Q_5 &= (\bar{s}_\alpha \gamma^\mu L b_\alpha) \sum_{q'} (\bar{q}'_\beta \gamma_\mu R q'_\beta), & Q_6 &= (\bar{s}_\beta \gamma^\mu L b_\alpha) \sum_{q'} (\bar{q}'_\alpha \gamma_\mu R q'_\beta), \\
Q_7 &= \frac{3}{2}(\bar{s}_\alpha \gamma^\mu L b_\alpha) \sum_{q'} e_{q'} (\bar{q}'_\beta \gamma_\mu R q'_\beta), & Q_8 &= \frac{3}{2}(\bar{s}_\beta \gamma^\mu L b_\alpha) \sum_{q'} e_{q'} (\bar{q}'_\alpha \gamma_\mu R q'_\beta), \\
Q_9 &= \frac{3}{2}(\bar{s}_\alpha \gamma^\mu L b_\alpha) \sum_{q'} e_{q'} (\bar{q}'_\beta \gamma_\mu L q'_\beta), & Q_{10} &= \frac{3}{2}(\bar{s}_\beta \gamma^\mu L b_\alpha) \sum_{q'} e_{q'} (\bar{q}'_\alpha \gamma_\mu L q'_\beta), \\
Q_{7\gamma} &= \frac{e}{8\pi^2} m_b \bar{s}_\alpha \sigma^{\mu\nu} R b_\alpha F_{\mu\nu}, & Q_{8g} &= \frac{g_s}{8\pi^2} m_b \bar{s}_\alpha \sigma^{\mu\nu} R T^a_{\alpha\beta} b_\beta G^a_{\mu\nu},
\end{aligned}
\tag{2}
$$

where α and β are color indices, and $L(R) = (1 \mp \gamma_5)$.

With the effective Hamiltonian given in Eq. (1), one can write the decay amplitudes for the relevant two-body hadronic $B \to M_1 M_2$ decays as

$$
\begin{aligned}
\mathcal{A}^{SM}(B \to M_1 M_2) &= \left\langle M_1 M_2 | \mathcal{H}_{eff}^{SM}(\Delta B = 1) | B \right\rangle \\
&= \sum_p \sum_i \lambda_p C_i^{SM}(\mu) \left\langle M_1 M_2 | Q_i(\mu) | B \right\rangle .
\end{aligned}
\tag{3}
$$

The essential theoretical difficulty for obtaining the decay amplitude arises from the evaluation of hadronic matrix elements $\langle M_1 M_2 | Q_i(\mu) | B \rangle$, for which we will employ the QCDF [25] throughout this paper. We will use the QCDF amplitudes of these decays derived in the comprehensive papers [15, 26] as inputs for the SM expectations.

2.1.2 SUSY effects in the decays

In SUSY extension of the SM with conserved R-parity, the potentially most important contributions to Wilson coefficients of penguin operators in the effective Hamiltonian arise from strong penguin and box diagrams with gluino-squark loops. They contribute to the FCNC processes because the gluinos have flavor-changing coupling to the quark and squark eigenstates. In general SUSY, we only consider these potentially large gluino box and penguin contributions and neglect a multitude of other diagrams, which are parametrically suppressed by small electroweak gauge coupling [19–22]. The relevant Wilson coefficients of $b \to su\bar{u}$ process due

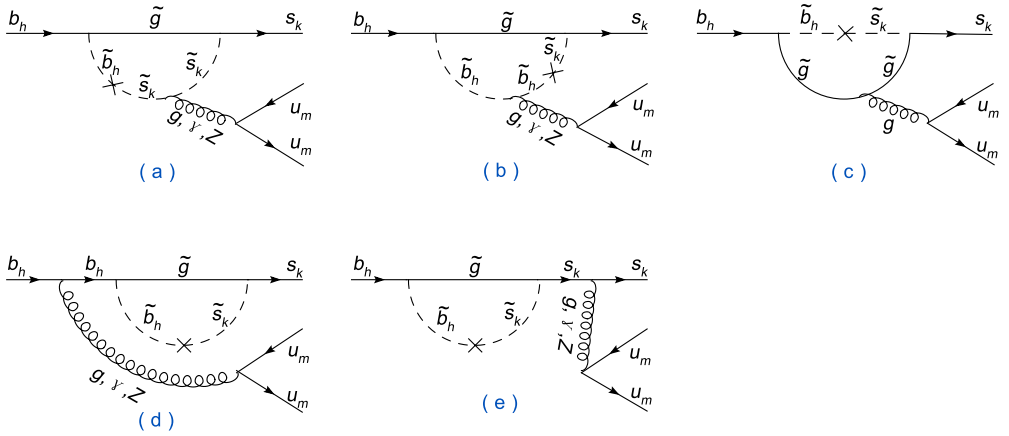

Figure 1: Penguin diagrams for $b \to su\bar{u}$ process with gluino exchanges at the first order in mass insertion, where $h, k, m = L, R$.

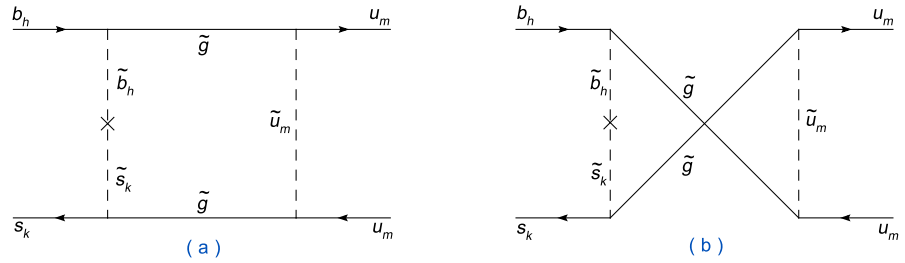

Figure 2: Box diagrams for $b \to su\bar{u}$ process with gluino exchanges at the first order in mass insertion, where $h, k, m = L, R$.

to the gluino penguin or box diagrams, which are shown in Fig. 1 and Fig. 2, respectively, involving the LL and LR insertions are given (at the scale $\mu \sim m_W \sim m_{\tilde{q}}$) by [19, 27–29]

$$
\begin{aligned}
C_3^{SUSY}(m_{\tilde{q}}) &= -\frac{\alpha_s^2(m_{\tilde{q}})}{2\sqrt{2}G_F\lambda_t m_{\tilde{q}}^2}\left(-\frac{1}{9}B_1(x) - \frac{5}{9}B_2(x) - \frac{1}{18}P_1(x) - \frac{1}{2}P_2(x)\right)(\delta^d_{LL})_{23}, \\
C_4^{SUSY}(m_{\tilde{q}}) &= -\frac{\alpha_s^2(m_{\tilde{q}})}{2\sqrt{2}G_F\lambda_t m_{\tilde{q}}^2}\left(-\frac{7}{3}B_1(x) + \frac{1}{3}B_2(x) + \frac{1}{6}P_1(x) + \frac{3}{2}P_2(x)\right)(\delta^d_{LL})_{23}, \\
C_5^{SUSY}(m_{\tilde{q}}) &= -\frac{\alpha_s^2(m_{\tilde{q}})}{2\sqrt{2}G_F\lambda_t m_{\tilde{q}}^2}\left(\frac{10}{9}B_1(x) + \frac{1}{18}B_2(x) - \frac{1}{18}P_1(x) - \frac{1}{2}P_2(x)\right)(\delta^d_{LL})_{23}, \\
C_6^{SUSY}(m_{\tilde{q}}) &= -\frac{\alpha_s^2(m_{\tilde{q}})}{2\sqrt{2}G_F\lambda_t m_{\tilde{q}}^2}\left(-\frac{2}{3}B_1(x) + \frac{7}{6}B_2(x) + \frac{1}{6}P_1(x) + \frac{3}{2}P_2(x)\right)(\delta^d_{LL})_{23}, \\
C_{7\gamma}^{SUSY}(m_{\tilde{q}}) &= \frac{8\pi\alpha_s(m_{\tilde{q}})}{9\sqrt{2}G_F\lambda_t m_{\tilde{q}}^2}\left[(\delta^d_{LL})_{23}M_4(x) - (\delta^d_{LR})_{23}\left(\frac{m_{\tilde{g}}}{m_b}\right)4B_1(x)\right], \\
C_{8g}^{SUSY}(m_{\tilde{q}}) &= -\frac{2\pi\alpha_s(m_{\tilde{q}})}{\sqrt{2}G_F\lambda_t m_{\tilde{q}}^2}\left[(\delta^d_{LL})_{23}\left(\frac{3}{2}M_3(x) - \frac{1}{6}M_4(x)\right)\right. \\
&\qquad \left. +(\delta^d_{LR})_{23}\left(\frac{m_{\tilde{g}}}{m_b}\right)\frac{1}{6}\left(4B_1(x) - 9x^{-1}B_2(x)\right)\right], \qquad (4)
\end{aligned}
$$

where $x \equiv m_{\tilde{g}}^2/m_{\tilde{q}}^2$, and the loop functions $B_i(x), P_i(x), M_i(x)$ can be found in Ref. [27]. For the RR and RL insertions, we have additional operators $\tilde{Q}_{i=3...6,7\gamma,8g}$ that are obtained by $L \leftrightarrow R$ in the SM operators given in Eq. (2). The associated Wilson coefficients $\widetilde{C}^{SUSY}_{i=3...6,7\gamma,8g}$ are determined by the expressions as above with the replacement $L \leftrightarrow R$. The remaining coefficients are either dominated by their SM ($C_{1,2}$) or electroweak penguins ($C_{7...10}$) and therefore small.

The SUSY Wilson coefficients at low energy $C_i^{SUSY}(\mu \sim m_b)$ can be obtained from $C_i^{SUSY}(m_{\tilde{q}})$ in Eq. (4) by using the renormalization group equation as discussed in Ref. [24]

$$C(\mu) = U_5(\mu, m_{\tilde{q}})C(m_{\tilde{q}}), \tag{5}$$

where C is the 6×1 column vector of the Wilson coefficients and $U_5(\mu, m_{\tilde{q}})$ [24] is the five-flavor 6×6 evolution matrix. The coefficients $C_{7\gamma}^{SUSY}$ and C_{7g}^{SUSY} at the $\mu \sim m_b$ scale are given by [30, 31]

$$\begin{aligned} C_{7\gamma}^{SUSY}(\mu) &= \eta^2 C_{7\gamma}^{SUSY}(m_{\tilde{q}}) + \frac{8}{3}(\eta - \eta^2) C_{8g}^{SUSY}(m_{\tilde{q}}), \\ C_{8g}^{SUSY}(\mu) &= \eta C_{8g}^{SUSY}(m_{\tilde{q}}), \end{aligned} \tag{6}$$

with $\eta = (\frac{\alpha_s(m_{\tilde{q}})}{\alpha_s(m_t)})^{\frac{2}{21}} (\frac{\alpha_s(m_t)}{\alpha_s(m_b)})^{\frac{2}{23}}$.

2.1.3 The total decay amplitudes

For the LL and LR insertions, the NP effective operators have the same chirality with the SM ones, so the total decays amplitudes can be obtained from the SM ones in Refs. [15, 26] by replacing

$$C_i^{SM} \to C_i^{SM} + C_i^{SUSY}. \tag{7}$$

For the RL and RR insertions, the NP effective operators have the opposite chirality with the SM ones, and we can get the corresponding decay amplitudes from the SM decay amplitudes by following replacements [32]

$$C_i^{SM} \to C_i^{SM} - \widetilde{C}_i^{SUSY}, \tag{8}$$

for $A(B_s \to K^- K^+)$ and $A_{0,\|}(B_s \to K^{*-} K^{*+})$, as well as

$$C_i^{SM} \to C_i^{SM} + \widetilde{C}_i^{SUSY}, \tag{9}$$

for $A(B_s \to K^{*-}K^+)$, $A(B_s \to K^-K^{*+})$ and $A_\perp(B_s \to K^{*-}K^{*+})$.

Then the total branching ratio reads

$$\mathcal{B}(B_s \to M_1M_2) = \frac{\tau_{B_s}|p_c|}{8\pi m_{B_s}^2} \left|\mathcal{A}(B_s \to M_1M_2)\right|^2, \tag{10}$$

where τ_{B_s} is the B_s lifetime, $|p_c|$ is the center of mass momentum in the center of mass frame of B_s meson.

In $B_s \to VV$ decay, the two vector mesons have the same helicity, therefore three different polarization states are possible, one longitudinal and two transverse, and we define the corresponding helicity amplitudes as $\mathcal{A}_{0,\pm}$. Transverse ($\mathcal{A}_{\parallel,\perp}$) and helicity ($\mathcal{A}_\pm$) amplitudes are related by $\mathcal{A}_{\parallel,\perp} = \frac{\mathcal{A}_+ \pm \mathcal{A}_-}{\sqrt{2}}$. Then we have

$$|\mathcal{A}(B_s \to VV)|^2 = |\mathcal{A}_0|^2 + |\mathcal{A}_+|^2 + |\mathcal{A}_-|^2 = |\mathcal{A}_0|^2 + |\mathcal{A}_\parallel|^2 + |\mathcal{A}_\perp|^2. \tag{11}$$

The longitudinal(transverse) polarization fraction $f_L(f_\perp)$ are defined by

$$f_{L,\perp}(B_s \to VV) = \frac{\Gamma_{L,\perp}}{\Gamma} = \frac{|\mathcal{A}_{0,\perp}|^2}{|\mathcal{A}_0|^2 + |\mathcal{A}_\parallel|^2 + |\mathcal{A}_\perp|^2}. \tag{12}$$

For the CP asymmetries (CPAs) of B_s meson decays, there is an additional complication due to $B_s^0 - \bar{B}_s^0$ mixing. There are four cases that one encounters for neutral B_s decays, as discussed in Ref. [33–36]:

- **Case (i)**: $B_s^0 \to f, \bar{B}_s^0 \to \bar{f}$, where f or $\bar{f}$ is not a common final state of B_s^0 and $\bar{B}_s^0$, for example $B_s^0 \to K^-\pi^+, K^-\rho^+, K^{*-}\pi^+, K^{*-}\rho^+$.

- **Case (ii)**: $B_s^0 \to (f = \bar{f}) \leftarrow \bar{B}_s^0$ with $f^{CP} = \pm f$, involving final states which are CP eigenstates, i.e., decays such as $B_s^0 \to K^-K^+$.

- **Case (iii)**: $B_s^0 \to (f = \bar{f}) \leftarrow \bar{B}_s^0$ with $f^{CP} \neq \pm f$, involving final states which are not CP eigenstates. They include decays such as $B_s^0 \to VV$, as the VV states are not CP eigenstates.

- **Case (iv)**: $B_s^0 \to (f\&\bar{f}) \leftarrow \bar{B}_s^0$ with $f^{CP} \neq f$, i.e., both f and $\bar{f}$ are common final states of B_s^0 and $\bar{B}_s^0$, but they are not CP eigenstates. Decays $B_s^0(\bar{B}_s^0) \to K^{*-}K^+, K^-K^{*+}$ belong to this case.

For case (i) decays, there is only direct CPA ($\mathcal{A}_{CP}^{dir}$) since no mixing is involved for these decays. For cases (ii) and (iii), their CPAs would involve $B_s^0 - \bar{B}_s^0$ mixing. The $\mathcal{A}_{CP}^{dir}$ and the mixing-induced CPA ($\mathcal{A}_{CP}^{mix}$) are defined as[1]

$$\mathcal{A}_{CP}^{k,dir}(B_s^0 \to f) = \frac{|\lambda_k|^2 - 1}{|\lambda_k|^2 + 1}, \quad \mathcal{A}_{CP}^{k,mix}(B_s^0 \to f) = \frac{2\mathrm{Im}(\lambda_k)}{|\lambda_k|^2 + 1}, \tag{13}$$

where $k = 0, \|, \perp$ for $B \to VV$ decays and $k = 0$ for $B \to PP, PV$ decays, in addition, $\lambda_k = \frac{q}{p}\frac{\mathcal{A}_k(\overline{B}^0 \to \bar{f})}{\mathcal{A}_k(B_s^0 \to f)}$ for CP case (i) and $\lambda_k = \frac{q}{p}\frac{\mathcal{A}_k(\overline{B}^0 \to f)}{\mathcal{A}_k(B_s^0 \to f)}$ for CP cases (ii) and (iii).

Case (iv) also involves mixing but requires additional formulas. Here one studies the four time-dependent decay widths for $B_s^0(t) \to f$, $\bar{B}_s^0(t) \to \bar{f}$, $B_s^0(t) \to \bar{f}$ and $\bar{B}_s^0(t) \to f$ [33–36]. These time-dependent widths can be expressed by four basic matrix elements [36]

$$\begin{aligned} g &= \langle f|\mathcal{H}_{eff}|B_s^0\rangle, \quad h = \langle f|\mathcal{H}_{eff}|\bar{B}_s^0\rangle, \\ \bar{g} &= \langle \bar{f}|\mathcal{H}_{eff}|\bar{B}_s^0\rangle, \quad \bar{h} = \langle \bar{f}|\mathcal{H}_{eff}|B_s^0\rangle, \end{aligned} \tag{14}$$

which determine the decay matrix elements of $B_s^0 \to f\&\bar{f}$ and of $\bar{B}_s^0 \to f\&\bar{f}$ at $t = 0$. We will also study the following observables

$$\mathcal{A}_{CP}^{k,dir}(B_s^0\&\bar{B}_s^0 \to f) = \frac{|\lambda_k'|^2 - 1}{|\lambda_k'|^2 + 1}, \quad \mathcal{A}_{CP}^{k,mix}(B_s^0\&\bar{B}_s^0 \to f) = \frac{2\mathrm{Im}(\lambda_k')}{|\lambda_k'|^2 + 1}, \tag{15}$$

$$\mathcal{A}_{CP}^{k,dir}(B_s^0\&\bar{B}_s^0 \to \bar{f}) = \frac{|\lambda_k''|^2 - 1}{|\lambda_k''|^2 + 1}, \quad \mathcal{A}_{CP}^{k,mix}(B_s^0\&\bar{B}_s^0 \to \bar{f}) = \frac{2\mathrm{Im}(\lambda_k'')}{|\lambda_k''|^2 + 1}, \tag{16}$$

with $\lambda_k' = \frac{q}{p}(h/g)$ and $\lambda_k'' = \frac{q}{p}(\bar{g}/\bar{h})$. The signature of CP violation is $\Gamma(\bar{B}_s^0(t) \to \bar{f}) \neq \Gamma(B_s^0(t) \to f)$ and $\Gamma(\bar{B}_s^0(t) \to f) \neq \Gamma(B_s^0(t) \to \bar{f})$, which means that $\mathcal{A}_{CP}^{k,dir}(B_s^0\&\bar{B}_s^0 \to f) \neq -\mathcal{A}_{CP}^{k,dir}(B_s^0\&\bar{B}_s^0 \to \bar{f})$ and/or $\mathcal{A}_{CP}^{k,mix}(B_s^0\&\bar{B}_s^0 \to f) \neq -\mathcal{A}_{CP}^{k,mix}(B_s^0\&\bar{B}_s^0 \to \bar{f})$.

2.2 $B_s^0 - \bar{B}_s^0$ mixing

The most general $B_s^0 - \bar{B}_s^0$ mixing is described by the effective Hamiltonian [38]

$$\mathcal{H}_{eff}(\Delta B = 2) = \sum_{i=1}^{5} C_i' Q_i' + \sum_{i=1}^{3} \widetilde{C}_i' \widetilde{Q}_i' + h.c., \tag{17}$$

with

$$Q_1' = (\bar{s}\gamma^\mu P_L b)_1 (\bar{s}\gamma_\mu P_L b)_1,$$

[1] We use a similar sign convention to that of [37] for self-tagging B_s^0 and charged B decays.

$$
\begin{aligned}
Q'_2 &= (\bar{s}P_L b)_1(\bar{s}P_L b)_1, \\
Q'_3 &= (\bar{s}P_L b)_8(\bar{s}P_L b)_8, \\
Q'_4 &= (\bar{s}P_L b)_1(\bar{s}P_R b)_1, \\
Q'_5 &= (\bar{s}P_L b)_8(\bar{s}P_R b)_8,
\end{aligned} \tag{18}
$$

where $P_{L(R)} = (1 \mp \gamma_5)/2$ and the operators $\widetilde{Q}'_{1,2,3}$ are obtained from $Q'_{1,2,3}$ by the exchange $L \leftrightarrow R$. The hadronic matrix elements, taking into account for renormalization effects, are defined as

$$
\begin{aligned}
\langle \bar{B}^0_s|Q'_1(\mu)|B^0_s\rangle &= \frac{2}{3}m^2_{B_s}f^2_{B_s}B_1(\mu), \\
\langle \bar{B}^0_s|Q'_2(\mu)|B^0_s\rangle &= -\frac{5}{12}m^2_{B_s}f^2_{B_s}S_{B_s}B_2(\mu), \\
\langle \bar{B}^0_s|Q'_3(\mu)|B^0_s\rangle &= \frac{1}{12}m^2_{B_s}f^2_{B_s}S_{B_s}B_3(\mu), \\
\langle \bar{B}^0_s|Q'_4(\mu)|B^0_s\rangle &= \frac{1}{2}m^2_{B_s}f^2_{B_s}S_{B_s}B_4(\mu), \\
\langle \bar{B}^0_s|Q'_5(\mu)|B^0_s\rangle &= \frac{1}{6}m^2_{B_s}f^2_{B_s}S_{B_s}B_5(\mu),
\end{aligned} \tag{19}
$$

with $S_{B_s} = \left(\frac{m_{B_s}}{\overline{m}_b(\overline{m}_b)+\overline{m}_s(\overline{m}_b)}\right)^2$.

The Wilson coefficients C'_i receive contributions from both the SM and the SUSY loops: $C'_i \equiv C'^{SM}_i + C'^{SUSY}_i$. In the SM, the $t-W$ box diagram generates only contribution to the operator Q'_1, and the corresponding Wilson coefficient C'^{SM}_1 at the m_b scale is [24]

$$
C'^{SM}_1(m_b) = \frac{G^2_F}{4\pi^2}m^2_W(V_{ts}V^*_{tb})^2\eta_{2B}S_0(x_t)[\alpha_s(m_b)]^{-6/23}\left[1+\frac{\alpha_s(m_b)}{4\pi}J_5\right], \tag{20}
$$

where $x_t = m^2_t/m^2_W$ and η_{2B} is the QCD correction.

In general SUSY models, there are new contributions to $B^0_s - \bar{B}^0_s$ mixing from the gluino-squark box diagrams, which are shown in Fig. 3, and the corresponding Wilson coefficients C'^{SUSY}_i (at the $m_{\tilde{q}}$ scale) are given by [19–22]

$$
\begin{aligned}
C'^{SUSY}_1(m_{\tilde{q}}) &= -\frac{\alpha^2_s}{216m^2_{\tilde{q}}}\left(24xf_6(x)+66\tilde{f}_6(x)\right)(\delta^d_{LL})^2_{23}, \\
C'^{SUSY}_2(m_{\tilde{q}}) &= -\frac{\alpha^2_s}{216m^2_{\tilde{q}}}204xf_6(x)(\delta^d_{RL})^2_{23}, \\
C'^{SUSY}_3(m_{\tilde{q}}) &= \frac{\alpha^2_s}{216m^2_{\tilde{q}}}36xf_6(x)(\delta^d_{RL})^2_{23}, \\
C'^{SUSY}_4(m_{\tilde{q}}) &= -\frac{\alpha^2_s}{216m^2_{\tilde{q}}}\left[\left(504xf_6(x)-72\tilde{f}_6(x)\right)(\delta^d_{LL})_{23}(\delta^d_{RR})_{23}-132\tilde{f}_6(x)(\delta^d_{LR})_{23}(\delta^d_{RL})_{23}\right],
\end{aligned}
$$

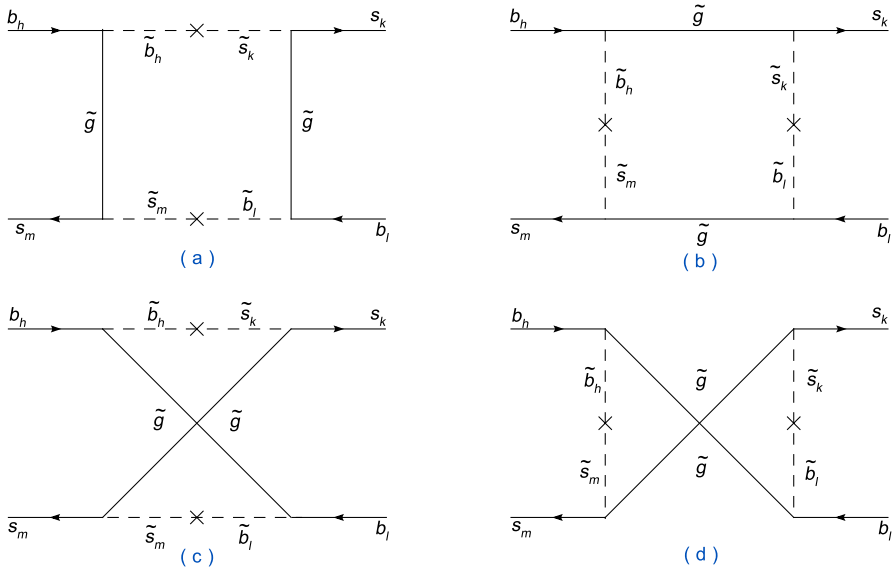

Figure 3: Feynman diagrams for $B_s^0 - \bar{B}_s^0$ mixing in mass insertion, where $h, k, l, m = L, R$.

$$C_5'^{SUSY}(m_{\tilde{q}}) = -\frac{\alpha_s^2}{216 m_{\tilde{q}}^2}\left[\left(24x f_6(x) + 120\tilde{f}_6(x)\right)(\delta^d_{LL})_{23}(\delta^d_{RR})_{23} - 180\tilde{f}_6(x)(\delta^d_{LR})_{23}(\delta^d_{RL})_{23}\right] \quad (21)$$

The loop functions $f_6(x)$ and $\tilde{f}_6(x)$ can be found in Ref. [27]. Other Wilson coefficients $\tilde{C}'^{SUSY}_{1,2,3}$ are obtained from $C'^{SUSY}_{1,2,3}$ by exchange of $L \leftrightarrow R$.

The SUSY Wilson coefficients at the m_b scale $C_i^{SUSY}(m_b)$ can be obtained by

$$C_r(m_b) = \sum_i \sum_s \left(b_i^{(r,s)} + \eta' c_i^{(r,s)}\right)\eta'^{a_i} C_s(m_{\tilde{q}}), \quad (22)$$

where $\eta' = \alpha_s(m_{\tilde{q}})/\alpha_s(m_t)$. The magic number a_i, $b_i^{(r,s)}$ and $c_i^{(r,s)}$ can be found in Ref. [38]. Renormalization group evolution of $\tilde{C}_{1,2,3}$ can be done in the same way as for $C_{1,2,3}$.

In terms of the effective Hamiltonian in Eq. (17), the mixing amplitude M_{12} read

$$M_{12} = \frac{\langle B_s^0|\mathcal{H}_{eff}(\Delta B = 2)|\bar{B}_s^0\rangle}{2m_{B_s}}. \quad (23)$$

In the SM, the off-diagonal element of the decay matrix $\Gamma_{12}^{s,SM}$ may be written as [39]

$$\Gamma_{12}^{s,SM} = -\frac{G_F^2 m_b^2}{8\pi M_{B_s}}(V_{cs}V_{cb}^*)^2\left[G(x_c)\langle B_s^0|Q_1|\bar{B}_s^0\rangle + G_2(x_c)\langle B_s^0|Q_2|\bar{B}_s^0\rangle + \sqrt{1-4x_c}\hat{\delta}_{1/m}\right], \quad (24)$$

where $x_c = m_c^2/m_b^2$, $G(x_c) = 0.030$ and $G_2(x_c) = -0.937$ at the m_b scale [39], the $1/m_b$ corrections $\hat{\delta}_{1/m}$ are given in Ref. [40], and $1/m_b^2$ corrections aren't considered since they are small [41]. It's important to note that, SUSY contributions can significantly affect M_{12}^s, but have little effect on Γ_{12}^s which is dominated by the CKM favored $b \to sc\bar{c}$ tree-level decays, hence $\Gamma_{12}^s = \Gamma_{12}^{s,SM}$ holds as a good approximation [5, 42, 43].

In general, the relevant CP violating phase between the $B_s^0 - \bar{B}_s^0$ amplitude and the amplitudes of the subsequent B_s^0 and $\bar{B}_s^0$ decay to a common final state could be expressed as [44]

$$\phi_s = \arg\left(-\frac{M_{12}^s}{\Gamma_{12}^s}\right). \tag{25}$$

The SM prediction for this phase is tiny, $\phi_s^{\rm SM} \approx 0.004$ [5]. The same additional contribution $\phi_s^{\rm NP}$ due to NP would change this observed phase, i.e., $\phi_s = \phi_s^{\rm SM} + \phi_s^{\rm NP}$. In case of sizable NP contributions, the following approximation is used: $\phi_s^{J/\psi\phi} \approx \phi_s \approx \phi_s^{\rm NP}$.

In this work, besides the CP violating phase $\phi_s^{J/\psi\phi}$, the experimental bounds of the following observables will be considered:

- the B_s mass difference: $\Delta M_s = 2\,|M_{12}^s|\,$;
- the B_s width difference [45]: $\Delta\Gamma_s = \frac{4|Re(M_{12}^s\Gamma_{12}^{s*})|}{\Delta M_s} \approx 2|\Gamma_{12}^s|\cos\phi_s$;
- the semileptonic CP asymmetry in B_s decays [46, 47]: $A_{SL}^s = {\rm Im}\left(\frac{\Gamma_{12}^s}{M_{12}^s}\right) = \frac{\Delta\Gamma_s}{\Delta M_s}\,\tan\phi_s$.

3 Numerical results and analysis

Now we are ready to present our numerical results and analysis. First, we will show our estimations in the SM with the theoretical input parameters listed in Table 4 of Appendix. Then, we will consider the SUSY effects with LL, RR, LR and RL four kinds of the MIs and constrain the relevant MI parameters with the experimental data of $B_s \to K^-K^+$, $B \to X_s\gamma$ and $B_s^0 - \bar{B}_s^0$ mixing. In each of the MI scenarios to be discussed, we will vary the MIs over the range $|(\delta_{AB}^d)_{23}| \leq 1$ to fully map the parameter space. We will consider the weak phases resided in the complex MI parameters $(\delta_{AB}^d)_{23}$ and appeared in the SUSY Wilson coefficients in Eq. (4) and Eq. (21), and these weak phases are odd under a CP transformation. Using the constrained parameter spaces, we will give the MI SUSY predictions for the branching ratios, the CPAs and the polarization fractions, which have not been measured yet in $B_s \to K^{(*)-}K^{(*)+}$ decays.

The numerical results in the SM are presented in second column of Table 1. For the decays, the detailed error estimations corresponding to the different types of theoretical uncertainties have been already studied in Refs. [15, 26, 48], and our SM results are consistent with the ones in Refs. [15, 26, 48]. For $B_s^0 - \bar{B}_s^0$ mixing, $\phi_s^{J/\psi\phi}$ and A_{SL}^s are precisely predicted in the SM, and

the uncertainties of ΔM_s and $\Delta\Gamma_s$ mainly arise from the non-perturbative quantity $f_{B_s}\sqrt{\hat{B}_{B_s}}$ and the CKM matrix elements.

Table 1: The theoretical predictions for $B_s \to K^{(*)-}K^{(*)+}$ decays and $B_s^0 - \bar{B}_s^0$ mixing based on general SUSY models with LR MI and $x = 9$. $\mathcal{B}$ and A_{SL}^s are in units of 10^{-6} and 10^{-2}, respectively. The corresponding SM predictions and relevant experimental data are also listed for comparison.

Observables	Experimental ranges at 95% C.L.	SM predictions	SUSY values with $(\delta^d_{LR})_{23}$ for $x = 9$
ΔM_s	$[17.53, 18.01]$	$[13.66, 24.82]$	$[17.53, 18.01]$
$\Delta\Gamma_s$	$[0.05, 0.33]$	$[0.10, 0.21]$	$[0.10, 0.21]$
ϕ_s	$[0.16, 2.84]$	$[0.034, 0.038]$	$[0.16, 0.52]$
A_{SL}^s	$[-0.04, 2.96]$	$[0.02, 0.05]$	$[0.11, 0.46]$
$\mathcal{B}(B_s \to K^-K^+)$	$[17.70, 35.30]$	$[9.20, 45.52]$	$[22.80, 35.30]$
$\mathcal{B}(B_s \to K^{*-}K^+)$		$[2.56, 23.19]$	$[2.39, 5.78]$
$\mathcal{B}(B_s \to K^-K^{*+})$		$[1.92, 6.72]$	$[9.73, 20.64]$
$\mathcal{B}(B_s \to K^{*-}K^{*+})$		$[3.56, 18.76]$	$[11.00, 45.40]$
$\mathcal{A}_{CP}^{mix}(B_s \to K^-K^+)$		$[0.25, 0.49]$	$[0.52, 0.79]$
$\mathcal{A}_{CP}^{mix}(B_s \& \bar{B}_s \to K^{*-}K^+)$		$[-0.34, 0.07]$	$[-0.09, 0.64]$
$\mathcal{A}_{CP}^{mix}(B_s \& \bar{B}_s \to K^-K^{*+})$		$[-0.44, 0.05]$	$[-0.14, 0.61]$
$\mathcal{A}_{CP}^{L,mix}(B_s \to K^{*-}K^{*+})$		$[0.70, 0.95]$	$[0.79, 0.98]$
$\mathcal{A}_{CP}^{dir}(B_s \to K^-K^+)$		$[0.00, 0.06]$	$[0.00, 0.07]$
$\mathcal{A}_{CP}^{dir}(B_s \to K^{*-}K^+)$		$[-0.08, 0.02]$	$[-0.17, 0.00]$
$\mathcal{A}_{CP}^{dir}(B_s \to K^-K^{*+})$		$[-0.10, 0.10]$	$[-0.04, 0.05]$
$\mathcal{A}_{CP}^{dir}(B_s \& \bar{B}_s \to K^{*-}K^+)$		$[-0.77, 0.27]$	$[0.05, 0.76]$
$\mathcal{A}_{CP}^{dir}(B_s \& \bar{B}_s \to K^-K^{*+})$		$[-0.24, 0.76]$	$[-0.76, -0.09]$
$\mathcal{A}_{CP}^{L,dir}(B_s \to K^{*-}K^{*+})$		$[-0.13, 0.21]$	$[-0.04, 0.10]$
$f_L(B_s \to K^{*-}K^{*+})$		$[0.36, 0.88]$	$[0.75, 0.96]$
$f_\perp(B_s \to K^{*-}K^{*+})$		$[0.06, 0.33]$	$[0.02, 0.13]$

Now we turn to the gluino-mediated SUSY contributions to $B_s \to K^{(*)-}K^{(*)+}$ decays and $B_s^0 - \bar{B}_s^0$ mixing in the framework of the MI approximation. The following experimental data

will be used to constrain relevant MI couplings [1, 2, 4, 10]

$$\begin{aligned}
\phi_s^{J/\psi\phi} &\in [0.20, 2.84] \text{ (at 95\% C.L.)}, && (26)\\
\Delta M_s &= 17.77 \pm 0.12, && (27)\\
\Delta\Gamma_s &= 0.19 \pm 0.07, && (28)\\
A_{SL}^s &= (1.46 \pm 0.75) \times 10^{-2}, && (29)\\
\mathcal{B}(B_s \to K^- K^+) &= (26.5 \pm 4.4) \times 10^{-6}. && (30)
\end{aligned}$$

In addition, the same set of the MI parameters also contribute to $B \to X_s\gamma$, which the gluino-mediated contribution can be found in Ref. [28]. Since the experimental measurement of $\mathcal{B}(B \to X_s\gamma)$ is in good agreement with the SM expectation, this implies very stringent constraints on NP models. We will also use [9]

$$\mathcal{B}(B \to X_s\gamma) = (3.55 \pm 0.24 \pm 0.09) \times 10^{-4} \quad (31)$$

to constrain the relevant MI parameters. Noted that above experimental data at 95% C.L. will be used to constrain the MI parameters.

3.1 LL insertion

Let's first consider the LL insertion. The effects of the LL insertions in $B_s \to K^{(*)-}K^{(*)+}$ decays are almost negligible because there is no the gluino mass enhancement, and $\mathcal{B}(B_s \to K^-K^+)$ given in Eq. (30) can not provide any useful constraint on $(\delta^d_{LL})_{23}$. The bound from A^s_{SL} is weaker than one from $\phi_s^{J/\psi}$, therefore A^s_{SL} also does not give any useful constraint when we consider all experimental data given in Eqs.(26-31) to constrain four kinds of the MI parameters. So we only impose the experimental constraints of $B_s^0 - \bar{B}_s^0$ mixing and $B \to X_s\gamma$ decay, which are shown in Eqs. (26-28) and Eq. (31), respectively, to restrict $(\delta^d_{LL})_{23}$.

The constrained spaces of $(\delta^d_{LL})_{23}$ for $m_{\tilde{q}} = 500$ GeV and different x values are demonstrated in Fig. 4, where the allowed parameter space for the MI is shown as dictated by the constraints imposed by $\mathcal{B}(B \to X_s\gamma)$ (yellow), $\Delta\Gamma_s$ (light gray), $\phi_s^{J/\psi\phi}$ (olive) and ΔM_s (pink). The wine region shows the allowed regions under the combined constraints of $\mathcal{B}(B \to X_s\gamma)$, $\mathcal{B}(B_s \to K^-K^+)$, $\Delta\Gamma_s$, ΔM_s, A^s_{SL} and $\phi_s^{J/\psi\phi}$. From Fig. 4, we see that the constrained regions are very sensitive to the values of x. For $x = 0.25, 1$, as shown in Fig. 4(a-b), the common allowed

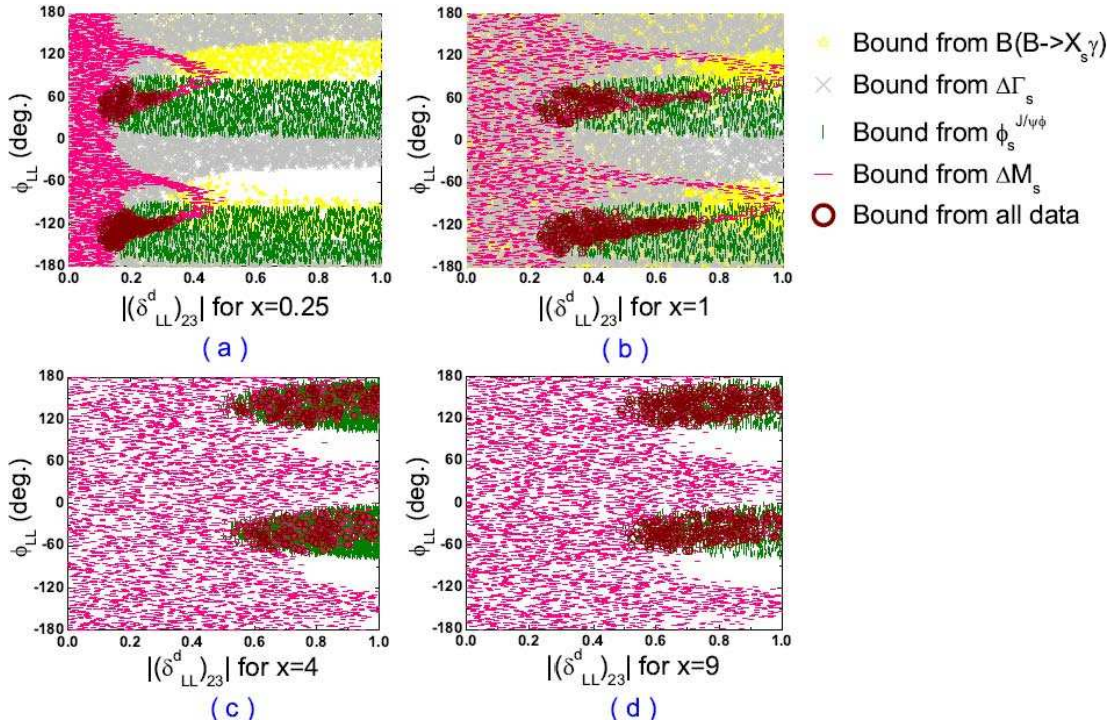

Figure 4: The allowed parameter spaces of the LL MI parameter constrained by $B_s \to K^- K^+$, $B \to X_s\gamma$ and $B_s^0 - \bar{B}_s^0$ mixing at 95% C.L. for the squark mass $m_{\tilde{q}} = 500$ GeV and the different values of x, and ϕ_{LL} denotes the mixing parameters weak phase.

regions are constrained by $\Delta\Gamma_s$, $\phi_s^{J/\psi\phi}$ and ΔM_s, nevertheless $\mathcal{B}(B \to X_s\gamma)$ does not give any further constraint. For $x = 4, 9$, we don't show the constraints from $\mathcal{B}(B \to X_s\gamma)$ in Fig. 4(c-d) since the whole region of $|(\delta^d_{LL})_{23}| \leq 1$ is allowed by the constraint of $\mathcal{B}(B \to X_s\gamma)$. As displayed in Fig. 4(c-d), the common allowed regions for $x = 4$ and 9 cases are constrained by $\phi_s^{J/\psi\phi}$ and ΔM_s, while $\Delta\Gamma_s$ does not give any further constraint. It is worth noting that, for $x = 0.25, 1, 4, 9$, the lower limit of $|(\delta^d_{LL})_{23}|$ is also constrained by $\phi_s^{J/\psi\phi}$ since its data are not consistent with its SM value at 95% C.L.. The relevant numerical bounds on $|(\delta^d_{LL})_{23}|$ with different x values are summarized in Table 2.

In Ref. [49], the constraint $|(\delta^d_{LL})_{23}| \leq 0.5$ for $m_{\tilde{g}}, m_{\tilde{q}} \leq 600$ GeV are derived from $\mathcal{B}(B \to X_s\gamma)$ and $\mathcal{B}(B \to X_s\ell^+\ell^-)$. Compared with the existed bound in [49], for $x = 0.25, 1$, our upper limits of $|(\delta^d_{LL})_{23}|$ are at the same order as the previous ones, while the lower limits of $|(\delta^d_{LL})_{23}|$ are also given by $\phi_s^{J/\psi\phi}$ at 95% C.L.. However, for $x = 4, 9$, our bounds on $|(\delta^d_{LL})_{23}|$ are greater than ones in Ref. [49]. Moreover, the bounds on the LL insertion with small tanβ by ΔM_s, $\phi_s^{J/\psi\phi}$, $\mathcal{B}(B \to X_s\gamma)$, $A_{CP}^{b\to s\gamma}$ and $S_{CP}^{\phi K}$ are also analyzed in detail in Ref. [50], for $m_{\tilde{q}} = 500$ GeV

Table 2: Bounds on the LL MI parameters from the measurements of $\mathcal{B}(B \to X_s\gamma)$, $\mathcal{B}(B_s \to K^-K^+)$, $\Delta\Gamma_s$, ΔM_s, A^s_{SL} and $\phi_s^{J/\psi\phi}$ at 95% C.L. for the squark mass $m_{\tilde{q}} = 500$ GeV.

x	0.25	1	4	9
$\lvert(\delta^d_{LL})_{23}\rvert$	$[0.10, 0.35]$	$[0.22, 0.76]$	$[0.54, 1.00]$	$[0.49, 1.00]$
ϕ_{LL}(deg.)	[29,79] [−154,−102]	[24,76] [−162,−101]	[112,170] [−69,−10]	[109,167] [−68,−12]

and $x = 1$ case, $\lvert(\delta^d_{LL})_{23}\rvert$ lies in $[0.42, 0.44] \cup [0.90, 0.95]$ with $\tan\beta = 3$ and lies in $[0.40, 0.65]$ with $\tan\beta = 10$.

The constrained LL MI shown in Fig. 4 allows that the theoretical prediction of ΔM_s lies in its 95% C.L. experimental range $[17.53, 18.01]$ for $x = 0.25, 1, 4, 9$. However, the ranges of $\phi_s^{J/\psi\phi}$, $\Delta\Gamma_s$ and A^s_{SL} are narrower than their 95% C.L. experimental ranges. For $x = 0.25, 1$, the constrained LL insertion coupling allows $\phi_s^{J/\psi\phi} \in [0.16, 1.26]$, $\Delta\Gamma_s \in [0.05, 0.20]$ and $A^s_{SL} \in [0.10, 1.00]$. For $x = 4, 9$, this coupling allows $\phi_s^{J/\psi\phi} \in [0.16, 0.52]$, $\Delta\Gamma_s \in [0.10, 0.20]$ and $A^s_{SL} \in [0.10, 0.47]$.

Furthermore, we also explore the LL insertion effects in $B_s \to K^{(*)-}K^{(*)+}$ decays. After satisfying all experimental data at 95% C.L. given in Eqs. (26-31), the constrained LL insertion will not provide significant contribution to $B_s \to K^{(*)-}K^{(*)+}$ decays. We find the upper limits of $\mathcal{B}(B_s \to K^{*-}K^{*+})$, $\mathcal{A}^{mix}_{CP}(B_s\&\bar{B}_s \to K^{*-}K^+, K^-K^{*+})$, $\mathcal{A}^{dir}_{CP}(B_s \to K^{*-}K^+)$ and $f_\perp(B_s \to K^{*-}K^{*+})$ are slightly decreased from their SM ranges by the constrained LL insertion. The lower limits of $\mathcal{A}^{L,dir}_{CP}(B_s \to K^{*-}K^{*+})$ and $f_L(B_s \to K^{*-}K^{*+})$ are slightly increased from their SM ranges by the constrained LL insertion. The allowed range of $\mathcal{A}^{L,mix}_{CP}(B_s \to K^{*-}K^{*+})$ is increased from its SM prediction $[0.70, 0.95]$ to [0.74,1.00] for $x = 0.25$, [0.77,0.99] for $x = 1$, [0.81,0.97] for $x = 4$ and [0.76,0.97] for $x = 9$, respectively, by the constrained LL insertion. While all observables of $B_s \to K^{(*)-}K^{(*)+}$ decays are insensitive to the modulus and weak phase of $(\delta^d_{LL})_{23}$.

3.2 RR insertion

For $B \to X_s\gamma$ decay, the situation of the RR insertion is very different from the LL one since the related NP amplitude (arising from right-handed currents) does not interfere with the SM one.

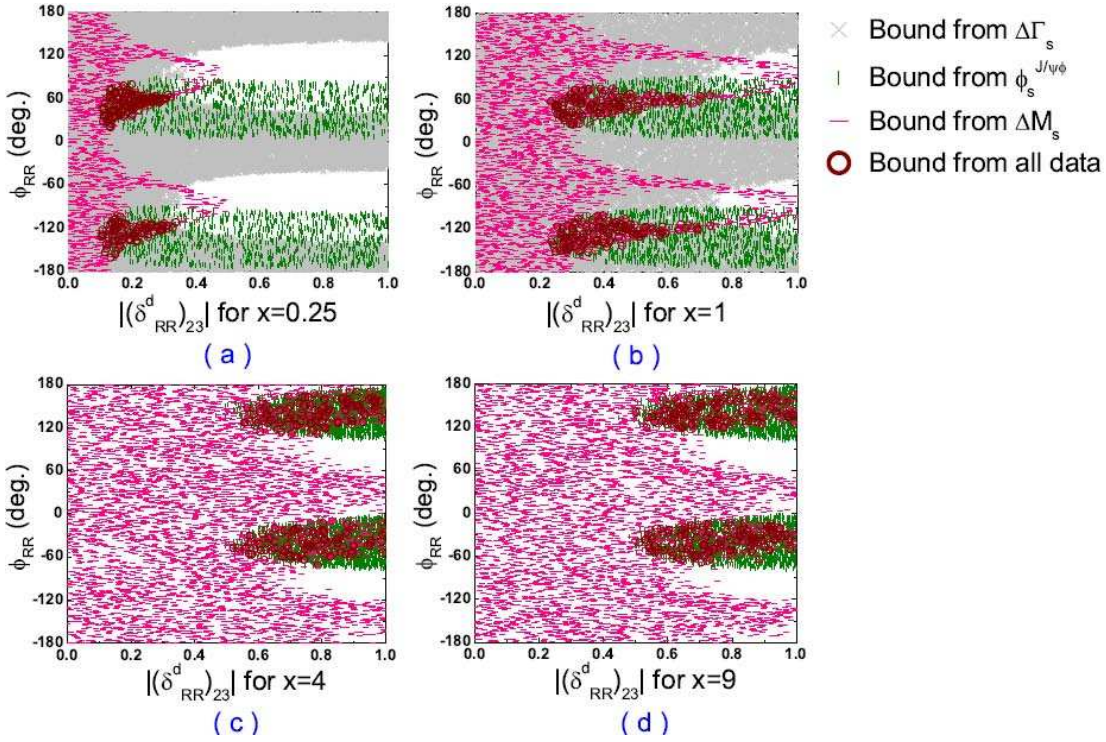

Figure 5: The allowed parameter spaces of the RR MI parameters constrained by $B_s \to K^-K^+$ decay and $B_s^0 - \bar{B}_s^0$ mixing at 95% C.L. for the squark mass $m_{\tilde{q}} = 500$ GeV and the different values of x.

Table 3: Bounds on the RR MI parameters from the measurements of $B_s \to K^-K^+$, $B \to X_s\gamma$ and $B_s^0 - \bar{B}_s^0$ mixing at 95% C.L. for the squark mass $m_{\tilde{q}} = 500$ GeV.

x	0.25	1	4	9
$\lvert(\delta^d_{RR})_{23}\rvert$	$[0.10, 0.34]$	$[0.23, 0.73]$	$[0.52, 1.00]$	$[0.50, 1.00]$
ϕ_{RR}(deg.)	[20,86] [−160,−104]	[25,75] [−153,−101]	[111,170] [−71,−11]	[118,170] [−69,−13]

Moreover, the effects of the RR insertion in $B_s \to K^-K^+$ are almost negligible also because of lacking the gluino mass enhancement in the decay. Therefore $(\delta^d_{RR})_{23}$ is strongly constrained by $B_s^0 - \bar{B}_s^0$ mixing. The constrained spaces of $(\sigma^d_{RR})_{23}$ by $B_s^0 - \bar{B}_s^0$ mixing for $m_{\tilde{q}} = 500$ GeV and different x values are demonstrated in Fig. 5, and the corresponding numerical ranges are summarized in Table 3. From Fig. 5 and Table 3, we can see that the allowed moduli and the allowed phase ranges of the RR parameters are also very sensitive to the values of x.

The bound of $(\delta^d_{RR})_{23}$ has been obtained in Refs. [49, 50]. The contributions of the product

$(\delta^d_{LL})_{23}(\delta^d_{RR})_{23}$ are also considered in Ref. [49], and they obtain $|(\delta^d_{RR})_{23}| \leq 0.8$ for $m_{\tilde{g}}, m_{\tilde{q}} \leq 600$ GeV from $\mathcal{B}(B \to X_s\gamma)$ and $\mathcal{B}(B \to X_s\ell^+\ell^-)$. In Ref. [50], the bounds on the RR insertion with small tanβ from ΔM_s, $\phi_s^{J/\psi\phi}$, $\mathcal{B}(B \to X_s\gamma)$, $A_{CP}^{b\to s\gamma}$ and $S_{CP}^{\phi K}$ are also analyzed in detail, for $m_{\tilde{q}} = 500$ GeV and $x = 1$ case, $|(\delta^d_{RR})_{23}|$ lies in $[0.36, 0.69]$ when tan$\beta = 3$, and there is no common range when tan$\beta = 10$.

The constrained RR insertion has the similar effects as the LL insertion on the observables of $B_s \to K^{(*)-}K^{(*)+}$ decays and $B_s^0 - \bar{B}_s^0$ mixing, and we will not show them here.

3.3 LR insertion

The effect of the LR insertion is very different from that of either LL or RR. In these decays, the LR MI only generates (chromo)magnetic operators $Q_{7\gamma,8g}$ and $\tilde{Q}_{7\gamma,8g}$. Especially, the LR insertion is more strongly constrained, since their contributions are enhanced by $m_{\tilde{g}}/m_b$ due to the chirality flip from the gluino in the loop. Thus even a small $(\delta^d_{LR})_{13}$ can have large effects in $B \to X_s\gamma$ and $B_s \to K^{(*)-}K^{(*)+}$ decays.

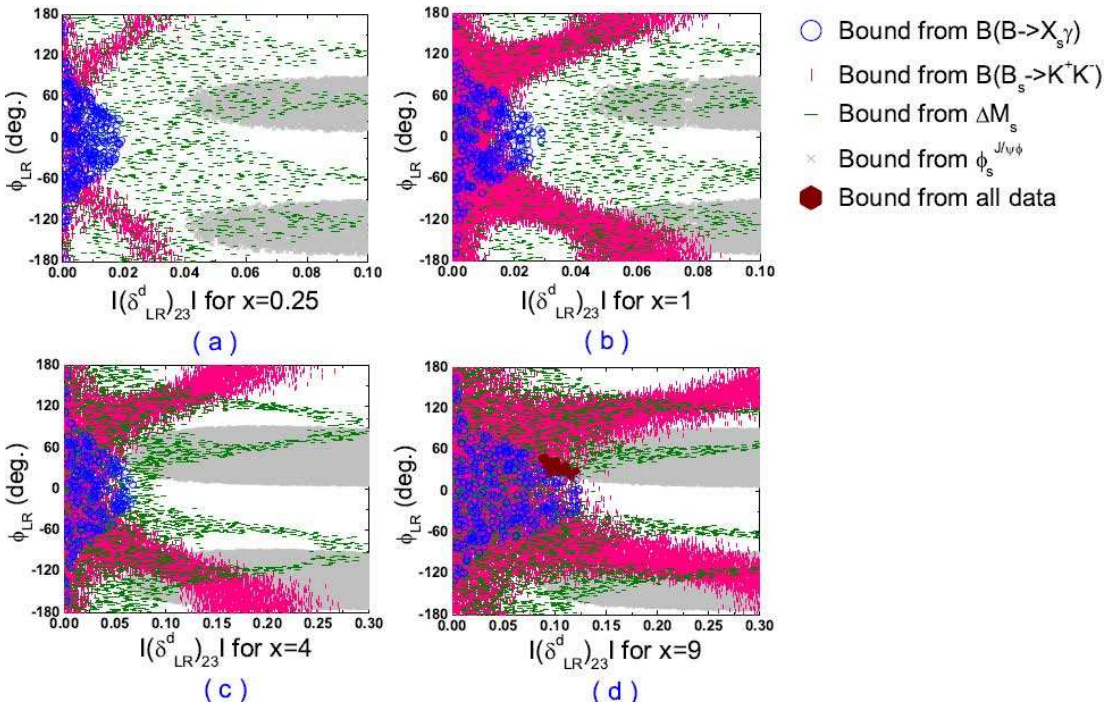

Figure 6: The allowed parameter spaces of the LR MI parameters constrained by $B_s \to K^-K^+$ decay and $B_s^0 - \bar{B}_s^0$ mixing at 95% C.L. for the squark mass $m_{\tilde{q}} = 500$ GeV and for the different values of x.

The constrained spaces of $(\delta^d_{LR})_{23}$ from $\mathcal{B}(B \to X_s\gamma)$, $\mathcal{B}(B_s \to K^-K^+)$ and $B^0_s - \bar{B}^0_s$ mixing for $m_{\tilde{q}} = 500$ GeV as well as different x are demonstrated in Fig. 6. $\Delta\Gamma_s$ can not provide any further constraint on $(\delta^d_{LR})_{23}$ and we will not show them in Fig. 6. From the figure, we can see that the allowed modulus of the LR MI parameter is very sensitive to the values of x, nevertheless the allowed phase range of the LR MI parameter is not changed much for different x. We find that $\mathcal{B}(B \to X_s\gamma)$ puts very strong constraints on the upper limit of $|(\delta^d_{LR})_{23}|$. And $\phi^{J/\psi}_s$ also puts very strong constraints on the lower limit of $|(\delta^d_{LR})_{23}|$ as well as the phase of $(\delta^d_{LR})_{23}$. For $x = 0.25, 1, 4$, the allowed spaces from $\mathcal{B}(B \to X_s\gamma)$, $\mathcal{B}(B_s \to K^-K^+)$ and ΔM_s are excluded by the constraint from $\phi^{J/\psi}_s$. For $x = 9$, there is small allowed space from $\mathcal{B}(B \to X_s\gamma)$, $\mathcal{B}(B_s \to K^-K^+)$, ΔM_s and $\phi^{J/\psi}_s$, and it is $|(\delta^d_{LR})_{23}| \in [0.08, 0.12] \ \cup \phi_{LR} \in [20^\circ, 51^\circ]$.

Previous bound $|(\delta^d_{LR})_{23}| \leq 0.012$ for $m_{\tilde{g}}, m_{\tilde{q}} \leq 600$ GeV has been obtained from the constraint of $\mathcal{B}(B \to X_s\gamma)$ in Ref. [49]. Comparing with Ref. [49], we can see that, as shown in Fig. 6 (a-c), the bounds for the cases of $x = 0.25, 1, 4$ from $\mathcal{B}(B \to X_s\gamma)$ and $\mathcal{B}(B_s \to K^-K^+)$ are stronger than the ones only from $\mathcal{B}(B \to X_s\gamma)$ although they are at the same order. While, as shown in Fig. 6 (d) for $x = 9$ case, the constraint from $\mathcal{B}(B \to X_s\gamma)$ is very strong and $\mathcal{B}(B_s \to K^-K^+)$ doesn't give any further constraint.

Next, we will explore the MI SUSY effects on other observables, which have not been (well) measured yet in $B_s \to K^{(*)-}K^{(*)+}$ decays and $B^0_s - \bar{B}^0_s$ mixing, by using the constrained parameter spaces of the LR for $x = 9$ case as shown in Fig. 6 (d). The numerical results for $B_s \to K^{(*)-}K^{(*)+}$ and $B^0_s - \bar{B}^0_s$ mixing are summarized in the third column of Table 1. For $x = 9$, the following comments are in order:

- The LR MI can great increase $\phi^{J/\psi}_s$ from the SM prediction range $[0.034, 0.038]$ to the SUSY prediction range $[0.16, 0.52]$, which is however near to the lower limit of the 95% C.L. measurement. The LR MI has been restricted by the experimental upper limit of $\mathcal{B}(B_s \to K^-K^+)$, and the allowed range of $\mathcal{B}(B_s \to K^-K^+)$ is significantly shrunken from its SM prediction $[9.20, 45.52] \times 10^{-6}$ to $[22.80, 35.30] \times 10^{-6}$ by the constrained LR insertion.

- The constrained LR could affect the branching ratios significantly. The allowed upper limit of $\mathcal{B}(B_s \to K^{*-}K^+)$ could be reduced from its SM prediction, and the allowed values of $\mathcal{B}(B_s \to K^-K^{*+}, K^{*-}K^{*+})$ are great increased by the constrained LR insertion.

The range of SUSY prediction of $\mathcal{B}(B_s \to K^- K^{*+})$ could differ from its SM expection significantly.

- The constrained LR insertion has great contributions to all mixing CPAs in $B_s \to K^{(*)-} K^{(*)+}$ decays, and all mixing CPAs could be largely enhanced. In addition, the constrained LR insertion could change $\mathcal{A}_{CP}^{dir}(B_s \& \bar{B}_s \to K^{*-} K^+, K^- K^{*+})$ a lot.

- The polarization fraction $f_L(B_s \to K^{*-} K^{*+})$ can be enhanced much by the constrained LR insertion.

For LR insertion with $x = 9$, we can present the distributions and correlations of $\mathcal{B}$, $\mathcal{A}_{CP}^{dir}$, $\mathcal{A}_{CP}^{mix}$, $f_{L,\perp}$ within the modulus or weak phase of the constrained LR MI parameter space in Fig.

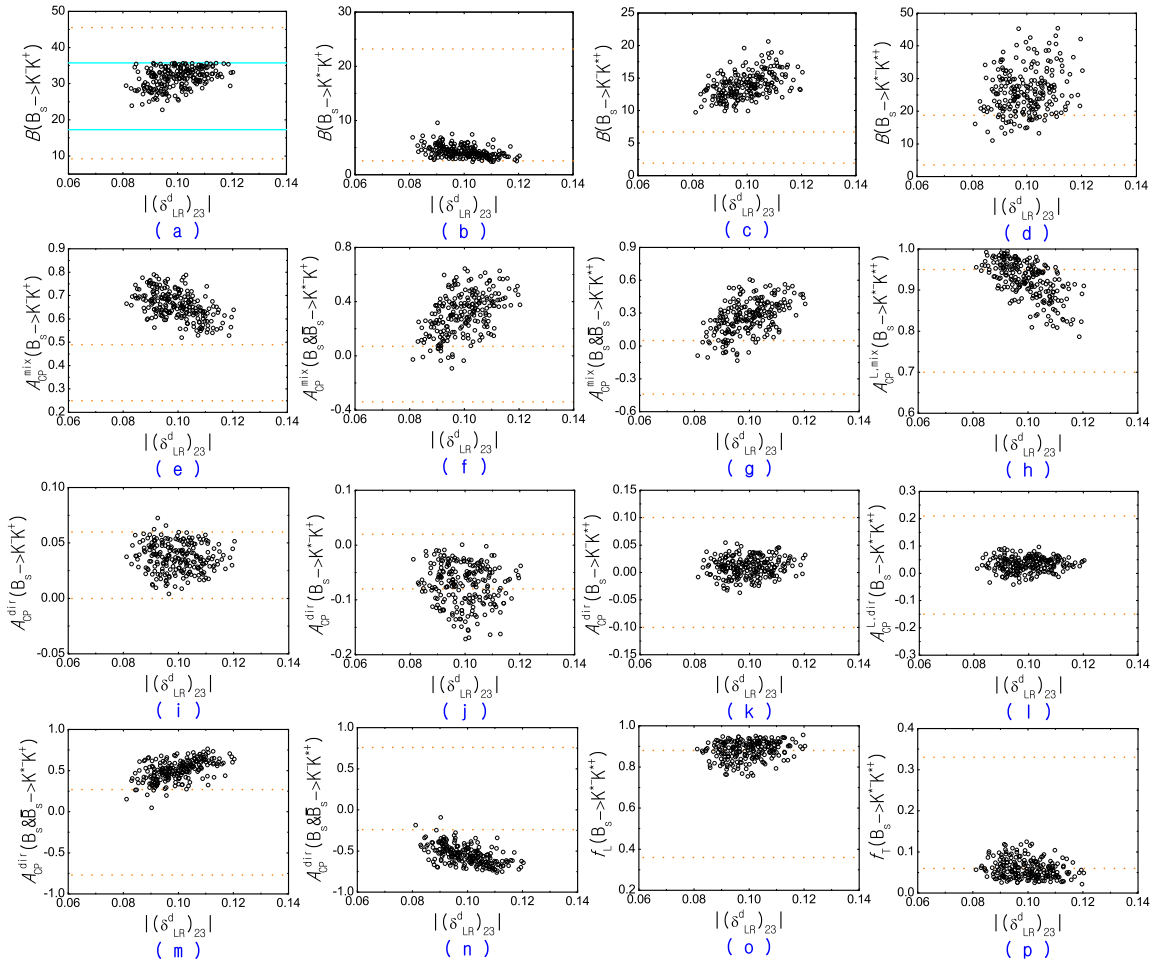

Figure 7: The effects of $\left|(\delta^d_{LR})_{23}\right|$ for $x = 9$ case in $B_s \to K^{(*)-} K^{(*)+}$ decays. $\mathcal{B}$ are in units of 10^{-6}. The orange horizontal dash-dot lines denote the limits of SM predictions, and the cyan horizontal solid lines represent the 2σ error bar of the measurements. (The same in Figs. 8).

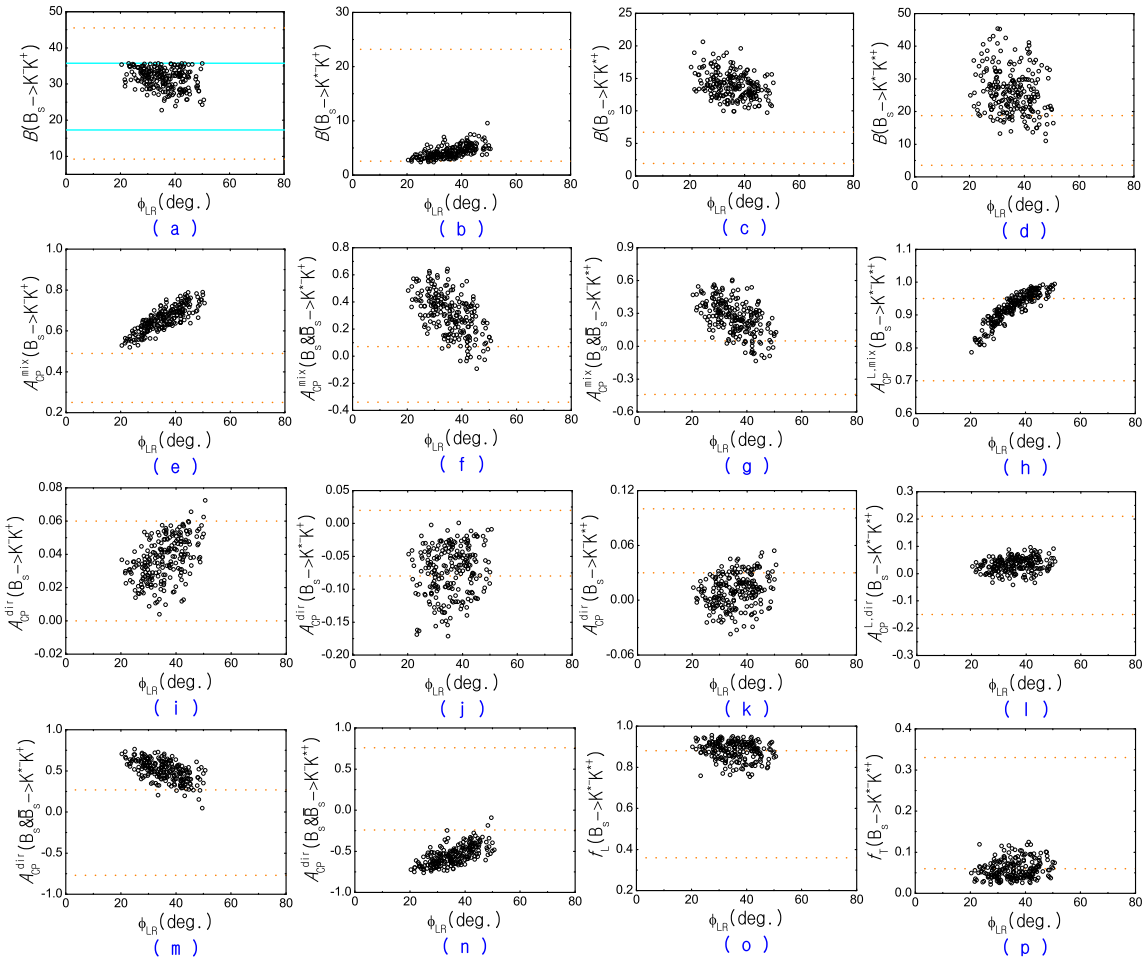

Figure 8: The effects of ϕ_{LR} for $x = 9$ case in $B_s \to K^{(*)-}K^{(*)+}$ decays.

6 (d) by two-dimensional scatter plots. The LR MI effects on all observables of $B_s \to K^{(*)-}K^{(*)+}$ decays are displayed in Figs. (7-8). Fig. 7 and Fig. 8 show the sensitivities of all observables to $|(\delta^d_{LR})_{23}|$ and ϕ_{LR}, respectively. In addition, for comparing conveniently, we show the SM bounds of these observables by orange horizontal dash lines and the limits of the measurements of $\mathcal{B}(B_s \to K^-K^+)$ at 95% C.L. by the cyan horizontal solid lines. From Fig. 7 (a-d) and Fig. 8 (a-d), one can find that $\mathcal{B}(B_s \to K^{*-}K^+, K^-K^{*+})$ have mild sensitivities to both $|(\delta^d_{LR})_{23}|$ and ϕ_{LR}, while $\mathcal{B}(B_s \to K^{*-}K^{*+})$ is insensitive to $|(\delta^d_{LR})_{23}|$ or ϕ_{LR}. As shown in Fig. 7(e-h) and Fig. 8(e-h), the LR insertion has positive effects on all four mixing CPAs, and they are sensitive to both $|(\delta^d_{LR})_{23}|$ and ϕ_{LR}. So the future measurement of any mixing CPA could further restrict both $|(\delta^d_{LR})_{23}|$ and ϕ_{LR}. Fig. 8 (i) and (k) show $\mathcal{A}^{dir}_{CP}(B_s \to K^-K^+, K^-K^{*+})$ are mildly sensitive to ϕ_{LR}. Fig. 7 (m-n) and Fig. 8 (m-n) display that $\mathcal{A}^{dir}_{CP}(B_s \& \bar{B}_s \to K^{*-}K^+, K^-K^{*+})$ are sensitive to both $|(\delta^d_{LR})_{23}|$ and ϕ_{LR}. As for the LR insertion effects on $f_L(B_s \to K^{*-}K^{*+})$

and $f_\perp(B_s \to K^{*-}K^{*+})$, we show them in Fig. 7 (o-p) and Fig. 8 (o-p), we can see $f_L(B_s \to K^{*-}K^{*+})$ and $f_\perp(B_s \to K^{*-}K^{*+})$ could be affected significantly by the LR MI.

3.4 RL insertion

The SUSY contributions of the RL insertion also pick up an $m_{\tilde{g}}/m_b$ enhancement relative to the SM. Compared to the LR case, the RL situation is very different since the related NP amplitude does not interfere with the SM one in $\mathcal{B}(B \to X_s\gamma)$. The RL insertion is much more strongly constrained by $\mathcal{B}(B \to X_s\gamma)$.

The constrained spaces of $(\delta^d_{RL})_{23}$ from $\mathcal{B}(B \to X_s\gamma)$, $\mathcal{B}(B_s \to K^-K^+)$ and $B^0_s - \bar{B}^0_s$ mixing for $m_{\tilde{q}} = 500$ GeV and different x are demonstrated in Fig. 9. $\Delta\Gamma_s$ can not provide any further constraint on $(\delta^d_{RL})_{23}$ which is not shown in Fig. 9. As shown in this figure, there is no common space from $\mathcal{B}(B \to X_s\gamma)$, $\mathcal{B}(B_s \to K^-K^+)$, ΔM_s and $\phi_s^{J/\psi}$ since $\mathcal{B}(B \to X_s\gamma)$ puts very strong constraints on the upper limits of $|(\delta^d_{RL})_{23}|$, roughly $|(\delta^d_{LR})_{23}| \leq 0.0057, 0.0086, 0.020, 0.036$ for $x = 0.25, 1, 4, 9$, respectively. So the RL insertion can't accommodate the current data of $\mathcal{B}(B \to X_s\gamma)$, $\mathcal{B}(B_s \to K^-K^+)$, ΔM_s and $\phi_s^{J/\psi}$ simultaneously.

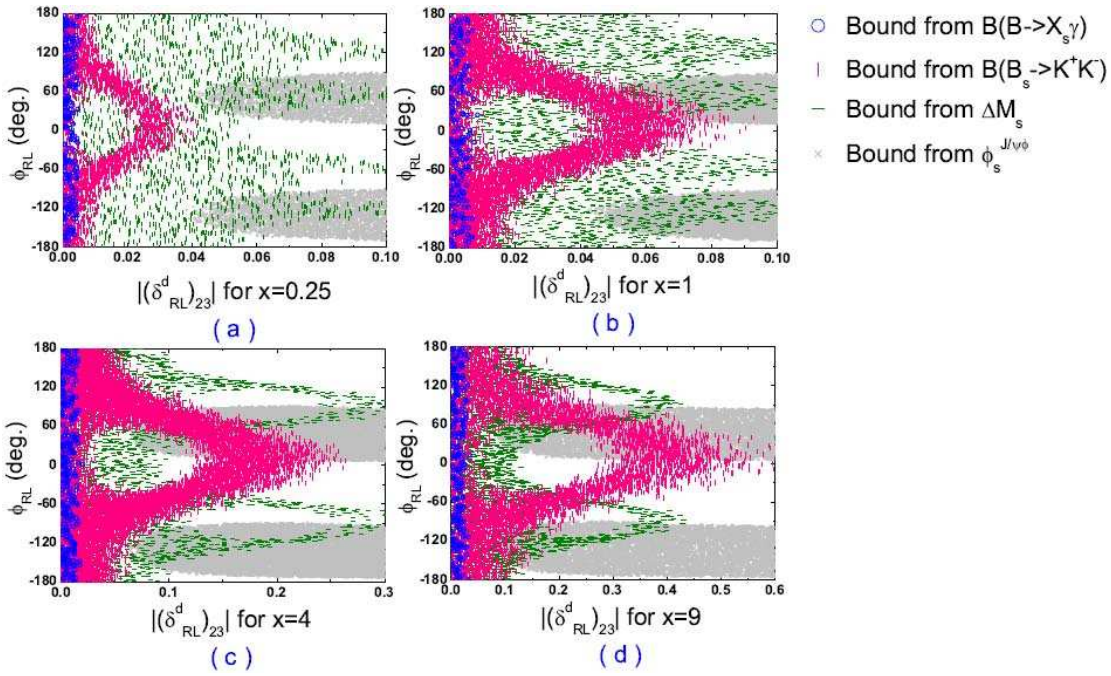

Figure 9: The allowed parameter spaces of the RL MI parameters constrained by $B_s \to K^-K^+$ decay and $B^0_s - \bar{B}^0_s$ mixing at 95% C.L. for the squark mass $m_{\tilde{q}} = 500$ GeV and the different values of x.

4 Conclusions

Motivated by the recent measurements from CDF and DØ collaborations, we have studied the gluino-mediated SUSY contributions to $B_s^0-\bar{B}_s^0$ mixing, $B_s \to K^{(*)-}K^{(*)+}$ and $B \to X_s\gamma$ decays with the MI approximation. Considering the theoretical uncertainties and the experimental error bars, we have obtained fairly constrained parameter spaces of LL, RR, LR and RL MIs from the present experimental data of $B_s^0 - \bar{B}_s^0$ mixing, $B_s \to K^-K^+$ and $B \to X_s\gamma$ decays. Furthermore, using the constrained MI parameter spaces, we have predicted the MI SUSY effects on the observables of four $B_s \to K^{(*)-}K^{(*)+}$ decays, which have not been measured yet.

For the LL and RR MIs, the strong constraint arises from $B_s^0 - \bar{B}_s^0$ mixing, and $\mathcal{B}(B_s \to K^-K^+)$ as well as $\mathcal{B}(B \to X_s\gamma)$ can not provide any further constraint on $(\delta^d_{LL,RR})_{23}$. We have found that, for $x = 0.25, 1, 4, 9$ cases, the constrained LL and RR MIs have little effect on the observables of $B_s \to K^{(*)-}K^{(*)+}$ decays. The upper limits of $\mathcal{B}(B_s \to K^{*-}K^{*+})$, $\mathcal{A}_{CP}^{mix}(B_s\&\bar{B}_s \to K^{*-}K^+, K^-K^{*+})$, $\mathcal{A}_{CP}^{dir}(B_s \to K^{*-}K^+)$ and $f_\perp(B_s \to K^{*-}K^{*+})$ are slightly decreased from their SM values. The lower limits of $\mathcal{A}_{CP}^{L,dir}(B_s \to K^{*-}K^{*+})$ and $f_L(B_s \to K^{*-}K^{*+})$ are slightly increased from their SM values. The allowed range of $\mathcal{A}_{CP}^{L,mix}(B_s \to K^{*-}K^{*+})$ is enlarged.

For the LR and RL MIs, $\mathcal{B}(B \to X_s\gamma)$ puts particularly strong constraints on the upper limits of $|(\delta^d_{LR,RL})_{23}|$, and $\phi_s^{J/\psi}$ also puts very strong constraints on the lower limits of $|(\delta^d_{LR,RL})_{23}|$ as well as the phases of $(\delta^d_{LR,RL})_{23}$. So only very narrow space of the LR MI for $x = 9$ case could explain the 95% C.L. experimental data of $\Delta\Gamma_s$, ΔM_s, A^s_{SL}, $\phi_s^{J/\psi\phi}$, $\mathcal{B}(B_s \to K^-K^+)$ and $\mathcal{B}(B \to X_s\gamma)$ simultaneously. We have found the constrained LR insertion for $x = 9$ still have sizable effects on all observables of $B_s \to K^{(*)-}K^{(*)+}$ decays except $\mathcal{A}_{CP}^{dir}(B_s \to K^-K^+)$. In addition, we have presented the sensitivities of the observables to the constrained LR parameter spaces in Figs. 7-8. We have found that all mixing CPAs of $B_s \to K^{(*)-}K^{(*)+}$ are very sensitive to both $|(\delta^d_{LR})_{23}|$ and ϕ_{LR}, moreover, $\mathcal{B}(B_s \to K^{*-}K^+, K^-K^{*+})$, $\mathcal{A}_{CP}^{dir}(B_s \to K^{*-}K^+)$, $\mathcal{A}_{CP}^{dir}(B_s\&\bar{B}_s \to K^{*-}K^+, K^-K^{*+})$ and $f_{L,\perp}(B_s \to K^{*-}K^{*+})$ have some sensitivities to $(\delta^d_{LR})_{23}|$ or ϕ_{LR}. So the future measurement of any mixing CPA could be very useful to shrink/reveal/rule out the relevant LR MI parameter space. The results could be useful for probing SUSY effects and searching direct SUSY signals at Tevatron and LHC in the near future.

Acknowledgments

The work was supported by National Science Foundation of P. R. China (Contract Nos. 11047145 and 11075059) and Project of Basic and Advanced Technology Research of Henan Province (Contract No. 112300410021).

Appendix: Input parameters

The input parameters are collected in Table 4. We have several remarks on the input parameters:

- Wilson coefficients: The SM Wilson coefficients C_i^{SM} are obtained from the expressions in Ref. [24].

- CKM matrix element: For the SM predictions, we use the CKM matrix elements from the Wolfenstein parameters of the latest analysis within the SM in Ref. [52], and for the SUSY predictions, we take the CKM matrix elements in terms of the Wolfenstein parameters of the NP generalized analysis results in Ref. [52].

- Masses of SUSY particles: When we study the SUSY effects, we will consider each possible MI $(\delta^d_{AB})_{23}$ for $AB = LL, LR, RL, RR$ only one at a time, neglecting the interferences between different insertions products, but keeping their interferences with the SM amplitude. We fix the common squark masses $m_{\tilde{q}} = 500$ GeV and consider four values of $x = 0.25, 1, 4, 9$ (i.e. $m_{\tilde{g}} = 250, 500, 1000, 1500$ GeV) in all cases.

Table 4: Values of the theoretical input parameters. To be conservative, we use all theoretical input parameters at 68% C.L. in our numerical results.

$m_W = 80.398 \pm 0.025$ GeV, $m_{B_s} = 5.366$ GeV, $m_{K^{*\pm}} = 0.892$ GeV, $m_{K^{\pm}} = 0.494$ GeV, $m_t = 171.3^{+2.1}_{-1.6}$ GeV, $\overline{m}_b(\overline{m}_b) = (4.20 \pm 0.07)$ GeV, $\overline{m}_s(2\text{GeV}) = (0.105^{+0.025}_{-0.035})$ GeV, $\tau_{B_s} = (1.472^{+0.024}_{-0.026})$ ps.	[51]
The Wolfenstein parameters for the SM predictions: $A = 0.810 \pm 0.013$, $\lambda = 0.2259 \pm 0.0016$, $\bar{\rho} = 0.154 \pm 0.022$, $\bar{\eta} = 0.342 \pm 0.014$. The Wolfenstein parameters for the SUSY predictions: $A = 0.810 \pm 0.013$, $\lambda = 0.2259 \pm 0.0016$, $\bar{\rho} = 0.177 \pm 0.044$, $\bar{\eta} = 0.360 \pm 0.031$.	[52]
$f_K = 0.160$ GeV, $f_{K^*} = (0.217 \pm 0.005)$ GeV, $f_{K^*}^{\perp} = (0.156 \pm 0.010)$ GeV, $A_0^{B_s \to K^*}(0) = 0.360 \pm 0.034$, $A_1^{B_s \to K^*}(0) = 0.233 \pm 0.022$, $A_2^{B_s \to K^*}(0) = 0.181 \pm 0.025$, $V^{B_s \to K^*}(0) = 0.311 \pm 0.026$, $F_0^{B_s \to K}(0) = 0.30^{+0.04}_{-0.03}$.	[53, 54]
$f_{B_s} = (0.245 \pm 0.025)$ GeV, $f_{B_s}\sqrt{\hat{B}_{B_s}} = 0.270 \pm 0.030$ GeV.	[55]
$\eta_{2B} = 0.55 \pm 0.01$.	[56]
$\alpha_1^K = 0.2 \pm 0.2$, $\alpha_2^K = 0.1 \pm 0.3$, $\alpha_1^{K^*} = 0.06 \pm 0.06$, $\alpha_2^{K^*} = 0.1 \pm 0.2$.	[15, 26]
$B_1^{(s)}(m_b) = 0.86(2)\left(^{+5}_{-4}\right)$, $B_2^{(s)}(m_b) = 0.83(2)(4)$, $B_3^{(s)}(m_b) = 1.03(4)(9)$, $B_4^{(s)}(m_b) = 1.17(2)\left(^{+5}_{-7}\right)$, $B_5^{(s)}(m_b) = 1.94(3)\left(^{+23}_{-7}\right)$.	[57]

References

[1] T. Aaltonen *et al.* [CDF Collaboration], Phys. Rev. Lett. **100**, 161802 (2008) [arXiv:0712.2397 [hep-ex]].

[2] V. M. Abazov *et al.* [DØ Collaboration], Phys. Rev. Lett. **101**, 241801 (2008) [arXiv:0802.2255 [hep-ex]].

[3] D. Tonelli [CDF Collaboration], arXiv:0810.3229 [hep-ex].

[4] CDF/DØ, $\Delta\Gamma$, β_s Combination Working Group, "Combination of DØ and CDF results on $\Delta\Gamma_s$ and the CP-violating phase $\beta_s^{J/\psi\phi}$ ", Note 5928-CONF, July 22, 2009.

[5] A. Lenz and U. Nierste, JHEP **0706**, 072 (2007) [arXiv:hep-ph/0612167].

[6] M. Bona *et al.*, arXiv:0906.0953 [hep-ph].

[7] L. Silvestrini, Nucl. Phys. Proc. Suppl. **185**, 41 (2008).

[8] M. Bona *et al.* [UTfit Collaboration], PMC Phys. A **3**, 6 (2009) [arXiv:0803.0659 [hep-ph]].

[9] D. Asner *et al.* [Heavy Flavor Averaging Group], arXiv:1010.1589 [hep-ex], and online update at http://www.slac.stanford.edu/xorg/hfag.

[10] V. M. Abazov *et al.* [DØ Collaboration], Phys. Rev. Lett. **105**, 081801 (2010) [arXiv:1007.0395 [hep-ex]].

[11] A. J. Lenz, AIP Conf. Proc. **1026**, 36 (2008) [arXiv:0802.0977 [hep-ph]].

[12] R. Louvot [Belle Collaboration], PoS EPS-HEP **2009**, 170 (2009) [arXiv:0909.2160 [hep-ex]].

[13] M. Morello [CDF Collaboration], Nucl. Phys. Proc. Suppl. **170**, 39 (2007) [arXiv:hep-ex/0612018].

[14] A. R. Williamson and J. Zupan, Phys. Rev. D **74**, 014003 (2006) [Erratum-ibid. D **74**, 03901 (2006)] [arXiv:hep-ph/0601214].

[15] M. Beneke and M. Neubert, Nucl. Phys. B **675**, 333 (2003) [arXiv:hep-ph/0308039].

[16] A. Ali *et al.*, Phys. Rev. D **76**, 074018 (2007) [arXiv:hep-ph/0703162].

[17] S. Baek, D. London, J. Matias and J. Virto, JHEP **0612**, 019 (2006) [arXiv:hep-ph/0610109].

[18] L. J. Hall, V. A. Kostelecky and S. Raby, Nucl. Phys. B **267**, 415 (1986).

[19] F. Gabbiani, E. Gabrielli, A. Masiero and L. Silvestrini, Nucl. Phys. B **477**, 321 (1996) [arXiv:hep-ph/9604387].

[20] F. Gabbiani and A. Masiero, Nucl. Phys. B **322**, 235 (1989).

[21] J. S. Hagelin, S. Kelley and T. Tanaka, Nucl. Phys. B **415**, 293 (1994).

[22] E. Gabrielli, A. Masiero and L. Silvestrini, Phys. Lett. B **374**, 80 (1996) [arXiv:hep-ph/9509379].

[23] R. M. Wang and Y. G. Xu, Phys. Rev. D **81**, 055011 (2010) [arXiv:1007.2943 [hep-ph]].

[24] G. Buchalla, A. J. Buras and M. E. Lautenbacher, Rev. Mod. Phys. **68**, 1125 (1996) [arXiv:hep-ph/9512380].

[25] M. Beneke, G. Buchalla, M. Neubert and C. T. Sachrajda, Phys. Rev. Lett. **83**, 1914 (1999) [arXiv:hep-ph/9905312]; Nucl. Phys. B **591**, 313 (2000) [arXiv:hep-ph/0006124]; Nucl. Phys. B **606**, 245 (2001) [arXiv:hep-ph/0104110].

[26] M. Beneke, J. Rohrer and D. Yang, Nucl. Phys. B **774**, 64 (2007) [arXiv:hep-ph/0612290].

[27] S. Baek, J. H. Jang, P. Ko and J. h. Park, Nucl. Phys. B **609**, 442 (2001) [arXiv:hep-ph/0105028].

[28] G. L. Kane *et al.*, Phys. Rev. D **70**, 035015 (2004) [arXiv:hep-ph/0212092].

[29] D. K. Ghosh, X. G. He, Y. K. Hsiao and J. Q. Shi, arXiv:hep-ph/0206186.

[30] A. J. Buras *et al.*, Nucl. Phys. B **566**, 3 (2000) [arXiv:hep-ph/9908371].

[31] X. G. He, J. Y. Leou and J. Q. Shi, Phys. Rev. D **64**, 094018 (2001) [arXiv:hep-ph/0106223].

[32] A. L. Kagan, arXiv:hep-ph/0407076.

[33] M. Gronau, Phys. Lett. B **233**, 479 (1989).

[34] J. Soto, Nucl. Phys. B **316**, 141 (1989).

[35] A. Ali, G. Kramer and C. D. Lu, Phys. Rev. D **59**, 014005 (1998) [arXiv:hep-ph/9805403].

[36] W. F. Palmer and Y. L. Wu, Phys. Lett. B **350**, 245 (1995) [arXiv:hep-ph/9501295].

[37] R. Fleischer, J. Phys. G **32**, R71 (2006) [arXiv:hep-ph/0512253].

[38] D. Becirevic *et al.*, Nucl. Phys. B **634**, 105 (2002) [arXiv:hep-ph/0112303].

[39] M. Beneke *et al.*, Phys. Lett. B **459**, 631 (1999) [arXiv:hep-ph/9808385]; A. Lenz, arXiv:hep-ph/9906317.

[40] M. Beneke, G. Buchalla and I. Dunietz, Phys. Rev. D **54**, 4419 (1996) [arXiv:hep-ph/9605259].

[41] A. Badin, F. Gabbiani and A. A. Petrov, Phys. Lett. B **653**, 230 (2007) [arXiv:0707.0294 [hep-ph]].

[42] X. G. He, B. Ren and P. C. Xie, arXiv:1009.3398 [hep-ph].

[43] I. I. Bigi, V. A. Khoze, N. G. Uraltsev and A. I. Sanda, in CP Violation, edited by C. Jarlskog (World Scientific, Singapore, 1988), p.175; J. L. Hewett, T. Takeuchi and S. Thomas, SLAC-PUB-7088 or CERN-TH/96-56; Y. Grossman, Y. Nir and R. Rattazzi, SLAC-PUB-7379 or CERN-TH-96-368; M. Gronau and D. London, Phys. Rev. D **55**, 2845 (1997).

[44] A. Lenz, Nucl. Phys. Proc. Suppl. **177**, 81 (2008) [arXiv:0705.3802 [hep-ph]].

[45] Y. Grossman, Phys. Lett. B **380**, 99 (1996) [arXiv:hep-ph/9603244].

[46] S. Baek and P. Ko, Phys. Rev. Lett. **83**, 488 (1999) [arXiv:hep-ph/9812229]; S. Baek and P. Ko, Phys. Lett. B **462**, 95 (1999) [arXiv:hep-ph/9904283]; L. Randall and S. f. Su, Nucl. Phys. B **540**, 37 (1999) [arXiv:hep-ph/9807377].

[47] Z. Ligeti, M. Papucci and G. Perez, arXiv:hep-ph/0604112; Y. Grossman, Y. Nir and G. Raz, arXiv:hep-ph/0605028.

[48] Y. G. Xu, R. M. Wang and Y. D. Yang, Phys. Rev. D **79**, 095017 (2009) [arXiv:0903.0256 [hep-ph]].

[49] W. Altmannshofer *et al.*, arXiv:0909.1333 [hep-ph].

[50] P. Ko and J. H. Park, Phys. Rev. D **80**, 035019 (2009) [arXiv:0809.0705 [hep-ph]].

[51] C. Amsler *et al.* [Particle Data Group], Phys. Lett. B **667**, 1 (2008) and 2009 partial update for the 2010 edition.

[52] M. Bona *et al.* (UT fitter Group), $http://www.utfit.org/$.

[53] P. Ball and R. Zwicky, Phys. Rev. D **71**, 014015 (2005) [arXiv:hep-ph/0406232]; P. Ball and R. Zwicky, Phys. Rev. D **71**, 014029 (2005) [arXiv:hep-ph/0412079].

[54] G. Duplancic and B. Melic, Phys. Rev. D **78**, 054015 (2008) [arXiv:0805.4170 [hep-ph]].

[55] V. Lubicz and C. Tarantino, Nuovo Cim. B **123**, 674 (2008) [arXiv:0807.4605 [hep-lat]].

[56] A. J. Buras, M. Jamin and P. H. Weisz, Nucl. Phys. B **347**, 491(1990); J. Urban *et al.*, Nucl. Phys. B **523**, 40 (1998).

[57] D. Bećirević *et al.*, JHEP **0204**, 025 (2002) [arXiv:hep-lat/0110091].